Implementation of a solar model and shadow plotting in the context of a 2D GIS

A validation based on radiometric measurements

Thomas Leduc, Xenia Stavropulos-Laffaille, Ignacio Requena-Ruiz

AAU-CRENAU, UMR 1563 CNRS/ECN/ENSAG/ENSAN
ENSA Nantes, 6 quai François Mitterrand, BP 16202, 44262 Nantes, France
thomas.leduc@crenau.archi.fr

ABSTRACT. The adaptation of public spaces to episodes of intense heat is now a major challenge for cities. With this in mind, this article presents a contribution aimed at delineating and handling the shadows on the ground or in a horizontal plane at a given height, whether it comes from buildings, street furniture or the tree cover. After a comparison with shadows obtained via two reference tools, we present two urban sites that mix shadows of different origins and, in addition, different indicators. The results of the simulations are compared with pyranometric surveys carried out on site. The aim of these indicators is to assist urban designers with solutions that make it possible to distinguish the respective shadow contributions, their annual evolution and potential spatial or temporal continuities.

RÉSUMÉ. L'adaptation des espaces publics aux épisodes de chaleur intense est désormais un défi majeur pour les villes. Dans cette optique, cet article présente une contribution qui a pour objet de délimiter et traiter l'ombre au sol ou dans un plan horizontal à une hauteur donnée, qu'elle provienne des bâtiments, du mobilier urbain ou du couvert arboré. Après une comparaison aux tracés des ombres obtenues via deux outils de référence, nous présentons deux sites urbains qui mélangent des ombres d'origines différentes ainsi que divers indicateurs. Les résultats des simulations sont comparés à des relevés pyranométriques réalisés sur site. L'objectif est ici d'aider les concepteurs urbains à trouver des solutions permettant de distinguer les contributions respectives des ombres, leur évolution annuelle et les éventuelles continuités d'ombres spatiales ou temporelles.

KEYWORDS: shade map, urban shade, tree canopy shade, urban microclimate, pyranometry, shade-based design.

MOTS-CLÉS : carte des ombres, ombre urbaine, ombre du couvert arboré, microclimat urbain, pyranométrie, conception basée sur l'ombre.

DOI:10.3166/rig31.241-263 © 2022 Lavoisier

1. Introduction

The warming stripes visualisation of climate data by Ed Hawkins (2018) show in a synthetic and intuitive way, the increasing frequency of extreme weather events (IPCC, 2022). Accordingly, our living environments suffer from rapid transformations (Hansen *et al.*, 2016) to which cities in so-called temperate regions are not prepared (Seager *et al.*, 2019). This effect concerns in particular the multiplication and intensification of heat waves in summer. The urban heat island (UHI)[1] phenomenon (Sobstyl *et al.*, 2018), which is a bioclimatic response specific to compact high-rise urban districts, amplifies these overheating, exposes populations to high health risks, and significantly alters living conditions in the built environment (Davis and Gertler, 2015). Both climate and demographic pressures constraint decision makers to organise urban lifestyles according to mitigation and adaptation strategies, which nowadays focus on how to cool down the urban space in short and mid-term.

Aram *et al*. (2019) consider four groups of urban cooling strategies: i) vegetative cover, ii) stack night ventilation, iii) water bodies and iv) modification of surface albedos. Authors such as (Demuzere *et al*., 2014; Gunawardena *et al*., 2017; Kabisch *et al.*, 2017; Lafortezza *et al*., 2018) consider strategies i) and iii) as a single set of Nature Based Solutions (NBSs). (Ruefenacht and Acero, 2017) propose more than 80 measures for mitigating UHI and highlight the relevance of shading as a "key measure to improve Outdoor Thermal Comfort (OTC) and mitigate UHI because it leads to the reduction of air and surface temperature and can therefore result in cooling benefits". Simultaneously, shading affects the pedestrians' thermal sensation and their adaptation strategies for dealing with heat stress situations. "This measure is relevant during daytime, especially around noon when the sun angles are at the highest." (Ruefenacht and Acero, 2017, p. 108). In this regard (Middel *et al*., 2016) enhance "the importance of solar access active management" to reduce thermal stress in public spaces of hot urban areas.

Regarding the benefits of shade provided by vegetation, tree growing is often promoted to modify radiative exchanges and airflow patterns at local scale (Redon *et al*., 2020). It minimises air and surface temperatures by intercepting incoming solar radiation, providing shade and cooling via evapotranspiration, which then improves thermal comfort significantly (Abdel-Aziz *et al.*, 2015; Coutts *et al*., 2016; Mullaney *et al*., 2015; Ruefenacht and Acero, 2017; Taha *et al*., 1991). Gillner *et al*. (2015) also observed this effect and noted "both Tilia and Corylus exhibit the highest rates of transpiration and highest LAD (Leaf Area Density) and are therefore the best options to reduce air temperature during summer days".

1. As (Ruefenacht and Acero, 2017) summarises: UHI "occurs because cities consume huge amounts of energy in electricity and fuel, have less vegetation to provide shade and cooling, and are built of materials that absorb and store energy from the sun".

By developing greening programs at city scale, decision makers have grasped the relevance of using large green spaces to mitigate the urban heat effects during hot periods: *e.g.* Plan d'action canopée of Montréal (CA), Parco Nord Milano (IT), Plan canopée of Grand Lyon (FR). However, the cooling effect of such green spaces on their surroundings, also called Green Space Cool Island, is strongly limited by its size (Emmanuel and Loconsole, 2015; Feyisa *et al*., 2014). As (Aram *et al*., 2019) explain, a park of at least 10 ha cools down from 1 to 2° C a perimeter of 350 m around it.

Martilli *et al*. (2020) state that the built environment is a tool for modifying local climates. As they suggest, if well controlled, this modification can be a source of thermal comfort in public space. According to the Coolscapes project (Stavropulos-Laffaille and Requena-Ruiz, 2021), this modification is an adaptation strategy to high temperatures in urban areas that starts at a very fine level: the scale of the pedestrian's immediate environment. Operating with local climate through design at this scale affects citizens' activities and behaviours in the public space during hot periods (Gehl, 2011; Whyte, 1980).

Ewing *et al.* (2006) proposed a conceptual framework of some 50 perceptual qualities in urban design. Their aim was to supply spatial designers with tools to quantify "the microscale streetscape features that affect the pedestrian experience" (Yin, 2017). They highlight bioclimatic aspects as crucial to anticipate future climate extreme events and mitigate their impacts on thermal comfort. Similarly (Aleksandrowicz *et al*., 2020) focus "on the provision of outdoor shade as a primary comfort indicator" for their methodology of evaluating microclimate summer conditions. Considering outdoor air temperature difficult to control, they observe that sunlight exposure in streets is easier to regulate since it is directly linked to design decisions. Therefore, they consider "outdoor shade as a primary comfort indicator".

We argue that a tool developed in the context of a standard GIS (based on shade index, tree canopy cover, etc.) can help in quantifying the microclimatic qualities of urban spaces revealing, for instance, sunlighted areas requiring shade intensification or, conversely, strategic shaded areas that deserve to be protected. The strictly geometric aspects of shading is essential in answering simple questions like where are located the "shadow fences"[2] generated by the urban environment at a given date and time? What is the fraction of space, for a predefined study area – which is in shadow for a given date and time? What is the tree canopy contribution to the total shade cover? What is the evolution of this contribution over the summer period, the crown remaining unchanged? Which areas are shaded for at least three hours on a hot summer day? To satisfy a constraint of temporal continuity, which areas are

2. We borrow this expression from (Knowles, 2003) to underline the fact that shadowing can also, in itself, generate constraints useful to the urban planner during a design phase (in reference to the solar envelope concept).

shaded for at least three consecutive hours on a hot summer day? Or even, do these areas guarantee spatial continuity in order to allow comfortable pedestrian mobility?

Simulation softwares such as Solene (Miguet and Groleau, 2002), Ladybug (Roudsari and Pak, 2013), UMEP-SOLWEIG (Lindberg *et al*., 2018) or ENVI-met[3], already allow shadow studies. Some of them (Solene and Ladybug) run as plugins of computer-aided design programs that do not offer the functionalities of GIS (power of synthesis of 2D maps, capacity to process large geographic areas, etc.) and require a particular expertise in architectural design. Therefore, their implementation by the geographic information departments of municipalities is difficult. On the contrary, UMEP-SOLWEIG has been embedded into a GIS. Nevertheless, they require digital surface and terrain models. In addition, the raster-based processes do not allow the shadow fences to be handled as simply as standard vector entities.

This article aims to highlight the interest of a specific vectorial development in a standard GIS to answer the questions mentioned above. After a presentation of the solar model and the treatment of mineral and vegetal shadows that we have implemented, we will present the mechanism for calculating multiple shadow overlaps. In the next section, we will highlight the interest of these developments in two different urban configurations of the Coolscapes research programme. To complete this methodological development, we will compare our simulation results with those obtained with computer-aided architectural design software tools and validate them using measuring of climate parameters and calculated thermal comfort indexes. Finally, we will discuss the contributions of our tool to a microclimate sensitive urban space design.

2. Method

Two main principles guide our methodological development: replicability and transportability on the one hand, and ease of implementation on the other. To guarantee these two principles, we use standard topographic datasets such as the ones provided by the IGN BD TOPO® database (December 2021 edition, IGN, 2021a) and a widely distributed free and open libraries (Geopandas by (Jordahl *et al.*, 2022), Shapely by (Gillies *et al*., 2021), and t4gpd by (Leduc, 2022)). It is noteworthy that the presented method of shadow simulation and mapping is potentially applicable at larger scales, *i.e.* district or city scale[4].

2.1. 3D processing in the context of 2D GIS

The sun path geometry and the delineation of the cast shadow generated by buildings and tree canopies are intrinsically three-dimensional urban issues. Our aim

3. ENVI-met is a German trademark (No. 304 73 896), https://www.envi-met.com/
4. It may then be appropriate to implement a coarse-grained parallel version using software solutions such as Python multiprocessing.

is to identify shaded areas that allow the city dweller to cool down; therefore, we simply delimit these areas on a horizontal plane at pedestrian level (in this case, we choose the ground plane). This simplifying hypothesis allows us, at the end of a 3D processing presented later on, to produce a classical 2D cartography in the context of a standard GIS.

2.2. Implementation of the sun path model

Pysolar (Stafford, 2020) and PyEphem (Rhodes, 2011) are Python implementations of ephemerides that allow estimating the trajectories and positions of the sun over time. To ensure consistency with the laboratory's simulation tools, we have implemented the ephemeris model of the Solene software in the context of our GIS simulation. A systematic comparison of the positions returned by Pysolar with those of our simulation shows that the respective solar heights differ by less than 1% on an annual average.

2.3. Shadow cast from a collection of right prisms

The topographic datasets employed here provide a 3D metric and vector description (structured in objects) of the elements of the territory and its infrastructure, usable on scales from 1:5,000 to 1:50,000. More precisely, this description consists of a set of polygons (sort of flat roof footprints) completed with an attribute equal to the height of the corresponding building. This twofold information allows us to generate a collection of right prisms each one representing a building in the urban model. The direction of the sun's beams being predetermined from the day and time of the simulation, it is then possible to i) calculate the ground shadow of each right prism, ii) and to proceed to a geometric union of all shadows.

2.4. Shadow cast from the tree canopies

Nantes Metropole's geographic information services provided us with a database of 75,156 trees in its conurbation. In addition to the point positions of each trunk, this data includes various attributes such as the height of the tree, the circumference of the trunk, the species of the tree, etc. In the first version of tree modelling, we developed three different crown models: the first is spherical, the second cylindrical and the third conical. Based on the tree attributes and positions as well as the crown model and the sunbeam direction, we have then implemented a ground shadow model (the projection of a sphere being an ellipse for example). As in the case of the building shadows, at the end of the process we proceed to the geometric union of all tree shadows in order to deal with possible overlaps.

2.5. Management of shadow overlaps over several (consecutive) hours

To identify areas in the shade for several hours (possibly consecutively), we need to make multiple geometric intersections, the combinatory of which are potentially substantial (for example, being in the shade for two hours can be translated multiply: 10 a.m.-11 a.m. and 3 p.m.-4 p.m., 1 p.m.-3 p.m., etc.). To deal efficiently with this issue and bypass these numerous intersections, we proceed in three steps using Shapely: i) geometric union (via the *unary_union* operator) of the shadow contours, ii) *polygonization* of the network of polylines thus produced, iii) for each polygon resulting from the *polygonization*, calculation of the number of enclosing shadow zones.

3. Case study and experimental setup

3.1. Focus on two distinct urban configurations in the city of Nantes, France

The first study site is located in the centre of Nantes (France), including parts of the Graslin District. This area consists of 13.6 ha, 293 building footprints representing a total floor area of about 6.4 ha, and 98 trees. Its altimetry varies from 6 to 30 metres and the average height of the buildings is about 15.7 m (with a standard deviation set at 5.8 m). The explained method is applied to this site with a special interest in the urban garden called “Cours Cambronne”. This classic French garden, lined with buildings and trees, covers about 0.9 ha and presents various shaded areas (from both surrounding buildings and 64 trees) that modify comfort indexes and citizens practices (*e.g.*, sitting places and trajectories). It is roughly 180 m long and 50 m wide. It also has the advantage of crossing shadows from the tree cover (rows of trees) and the building environment, all on a relatively flat ground.

The second study site is an ordinary urban configuration around a plaza at the intersection of a boulevard and two streets. This urban fragment is contained within a recently renovated district. It embodies an experimental “freshness device” that was recently deployed by the municipality. With a surface area of 0.4 ha, it contains 24 trees mainly grouped in its northern and southern ends. In contrast to the first study site, which is oriented exclusively from south-west to north-east, this configuration is less homogeneous with a main north-south orientation.

3.2. Experimental setup: model building

In order to test our methodological proposal and respond to the research questions, we have defined several parameters as follows. Regarding the choice of representative dates and times for the annual sunshine simulation, we have chosen the 1st, 11th and 21st of each month. For each of these days, we have made a calculation with an hourly time step from 10 a.m. to 4 p.m. UTC. This choice of

dates is identical for both study sites. Regarding the choice of a representative summer day, we opted for July 21st. Regarding the tree modelling in the first study site, after empirical evaluation on the site, we chose a cylindrical crown model with two distinct parameterizations. Eight trees in the Courtyard have a total height of 15 m, a crown height of 10 m and a crown radius equal to 5 m. The rest of the trees are modelled with a total height of 9 m, a crown height of 6 m and a crown radius of 3 m. The trees at the second site were less uniform, so a site survey was carried out to reflect the variety of possible crown configurations. It is noteworthy that although the trees in the two sites are deciduous, we do not consider the change in the crown due to seasonality.

3.3. Experimental setup: mobile climate measurements

To validate our simulation model of solar trajectories and shadow plots, we have decided to compare the shadow plots with in situ experimental measurements. We have retrieved data from the research project Coolscapes dedicated to the study of urban cool spots throughout the cities (Requena-Ruiz *et al*., 2022). In this context, we have developed a mobile climate measuring station for observing detailed microclimate conditions at body level. Robust scientific sensors with a very short response time are mounted on a reconfigured bike trailer. The measuring height is around 1.1 m, corresponding to the centre of the human body's gravity when standing (Johansson *et al*., 2014). It is composed by sensors for measuring air temperature (2 thermocouples and 1 thermohygrometer), relative humidity (1 thermohygrometer), wind direction and speed (1 ultrasonic anemometer), and long-and short-wave solar radiation of the pedestrians' three-dimensional environment (3 Hukseflux 4-component Net Radiometers NR01). The measuring frequency is 2 sec, 10 sec and 15 min.

The spatialisation of mobile measurements requiring high precision, we opted for a foot mounted inertial sensing system (Inertial Elements) developed for high-precision pedestrian navigation (Gupta *et al*., 2015). It is based on high-performance motion sensor platforms (IMUs) using "Sensor Fusion" and "Array Signal Processing methods".

Measuring campaigns for the Coolscapes project in the Cambronne site took place on September 4th, 9th, 11th, 14th and 16th.

4. Experimental verification

4.1. Comparison of shadows in the context of a CAAD software

The objective of this section is to use the solar model and the shadow engine implemented natively in the SketchUp software, to compare the shadows computed by the t4gpd plugin in the context of a GIS with those of a tool widely used by architectural practitioners. For that, we first import the building footprints and tree

positions to build the corresponding 3D model using the SketchUp *pushpull* mechanism. We then import the shadow polygons produced by our simulations (through the SHP file format) and compare them visually to the shadows produced by the SketchUp shadow engine. Figure 1 shows that these two shadow features match satisfactorily.

Figure 1. Comparison of the native SketchUp shadow features (in grey) with those from the t4gpd plugin (red polylines), on July 21 at 10 a.m. UTC

4.2. Comparison with the Urban Multi-scale Environmental Predictor (UMEP)

As the verification proposed in the previous section is purely visual, we suggest comparing our simulation results with those of the UMEP reference tool. Indeed, the latter embeds the shadow generator plugin capable of generating shadow plots from building, ground or even vegetation digital surface models, in the QGIS context (QGIS Association, 2022). In order to use UMEP's "Daily Shadow Pattern" functionality, we first had to generate a digital terrain model, a digital model of the built-up surfaces, and a raster model of the tree canopy. We used a metric precision raster model such as the one proposed by the RGE Alti® (IGN, 2021b) to stick as closely as possible to the building layouts. Figure 2 shows the relatively good correlation of the raster shadows produced by UMEP with the vector traces from our simulations.

Table 1. Comparison of shadow-covered area measurements (in m²) assessed via the UMEP software vs. via the t4gpd plugin, on July 21st

	10 a.m.	11 a.m.	12 a.m.	1 p.m.	2 p.m.	3 p.m.
UMEP	35,498.6	29,062.9	27,838.8	27,677.2	28,900.2	36,852.8
T4gpd	33,694.2	29,093.6	28,036.8	27,533.8	28,560.2	36,161.6
Deviation	5.2 %	0.1 %	0.7 %	5.2 %	1.2 %	1.9 %

To go beyond this visual comparison, we measured the shadow-covered areas respectively produced by UMEP and our simulation tool at different times on 21st July. Table 1 shows variations ranging from 0.1% to 5.2%. Although this comparative analysis does not formally validate our simulation tool, it reinforces our ability to produce consistent results with the UMEP reference tool.

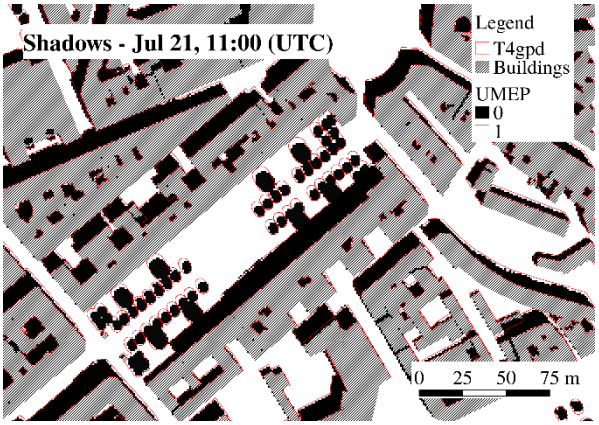

Figure 2. Comparison of the shadows from the UMEP Shadow generator black pixels) with those from the t4gpd plugin (red polylines)

4.3. Comparison with short-wave radiation values measured on site

In order to test the validity of our shadow plots in a horizontal plane located at 1.10 m from the ground (the height at which the sensors are anchored on the measurement trailer), we wished to compare them with solar radiation measurements at a set of equally distributed points along the trajectory.

The measurements on the Cambronne site were taken on five days during September 2020. Depending on the weather, three, four or five passages were carried out each day, at a (relatively) fixed time, in order to highlight possible permanencies or specificities related to the spatial configuration of the places. The measurements presented here are those of pyranometers of the SR01 type facing the sky. The unit of measurement is W/m^2.

As shown on the map and plot in Figure 3, the shadow cast by the statue of General Cambronne and its plinth in the middle of the square has an obvious (but temporary) impact on the radiometric measurement at point 32. To highlight this correlation, we have chosen to represent in red, on the map on the left-hand side of Figure 3, all the sensors whose pyranometry measurement directed towards the sky is higher than 200 W/m^2. This value, assumed here as a hypothesis, has been stated as the threshold for encouraging staying activities in the public space during

summer; which is related to thermally comfortable situations (Cui *et al.*, 2021). In contrast, in the plot on the right-hand side of Figure 3, the horizontal segments in red represent positions in the sun in the simulation plane located at a height of 1.10 m and those in blue are associated with positions in the shade.

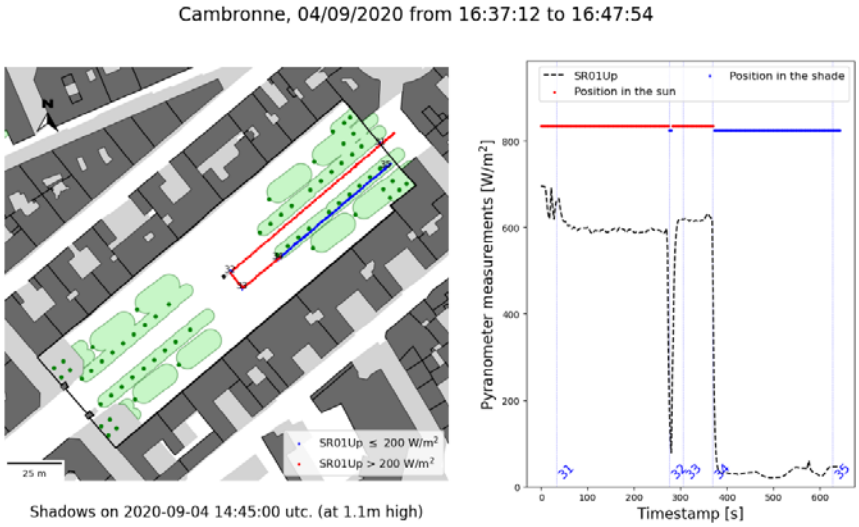

Figure 3. Comparison of the shadow plots obtained by the simulation with pyranometric measurements carried out in situ.

To go beyond this visual comparison and to be able to characterise all the measurements carried out with regard to our simulations, we have decided to transpose an approach commonly used in epidemiology or in the theory of signal detection. This involves measuring the intrinsic validity of a hypothesis by means of sensitivity and specificity indicators (Altman and Bland, 1994). The results presented in Table 2 correspond to the following hypothesis: "a sensor in the shade has a SR01Up less than or equal to 200 W/m^2".

First, we can see that some radiometry measurements correlate very well with the simulation. For instance, this is the case for the runs carried out on September 11 at 4.30 p.m., on September 14 at noon or 4.30 p.m. or on September 16 at noon, 1.30 p.m. and 4.30 p.m.). However, sometimes the differences between the measurement and the simulation are very large. This was the case, for example, on September 9 after 4.30 p.m., with radiometry measurements all below 200 W/m^2, typical of an overcast situation. As in the simulation tool we present here, our shadow plots are theoretical; they do not integrate this cloudiness, which strongly disturbs the radiometry measurements.

Table 2. Measure of the intrinsic validity of the following hypothesis "a sensor in the shade has a SR01Up less than or equal to 200 W/m2". Here TP stands for "True positive", TN for "True negative", FP for "False positive" and FN for "False negative"

Date	In shade	SR01 <200 W/m^2	Delta	TP	TN	FP	FN	Sens.	Spec.
04/9 13:38	40,4	11,1	29,3	11	25	64	0,3	97,6	27,7
04/9 15:10	28,9	11,9	17	7,7	31	57	4,2	64,6	35,6
04/9 16:37	35,1	42,9	-7,7	43	0,3	57	0	100	0,5
09/9 12:10	82,9	48,9	33,9	45	36	15	3,8	92,3	70,4
09/9 13:40	42,3	11,4	30,9	10	29	60	1	91,4	32,4
09/9 15:06	28,3	7,8	20,5	4,6	17	76	3,2	59,3	17,9
09/9 16:35	35,1	100	-65	29	0	0	72	28,5	0
11/9 12:11	83,1	63	20	61	22	15	2,3	96,4	59,7
11/9 13:42	42,8	31,7	11,1	25	25	44	6,3	80	35,9
11/9 15:09	28,1	7,9	20,2	6,9	20	72	0,9	88	21,8
11/9 16:36	35,2	32,6	2,6	33	1,7	66	0	100	2,5
14/9 12:06	83,4	80	3,4	76	8,3	12	4,3	94,6	41,4
14/9 13:36	43,4	30,6	12,8	22	20	50	8,6	71,9	28,4
14/9 15:07	27,7	7,2	20,5	6,9	16	77	0,3	96	17
14/9 16:37	35,2	30,6	4,6	30	2,3	67	0,3	98,9	3,3
14/9 18:05	69,6	76,6	-7	74	0,3	23	2,7	96,4	1,3
16/9 12:09	83,7	84,2	-0,5	81	6,5	9,4	3,6	95,7	41
16/9 13:37	43,8	42,3	1,6	35	15	42	7,1	83,2	26,7
16/9 15:07	27,4	7,5	19,9	7,5	17	75	0	100	18,8
16/9 16:36	35,2	34,4	0,8	34	3,9	62	0	100	5,9

5. Application to two distinct urban configurations in the city of Nantes

5.1. Shade ratios

5.1.1. Shade ratio at a given date and time

The first very simple application consists, in delineating the ground shadow due to the tree canopy and the built environment for a given territory, date and time. On July 21 at 12 a.m. (UTC), the surrounding buildings and 64 trees enclosed in the study site named Cours Cambronne thus produce a ground shade of approximately 0.46 ha, i.e. approximately 46.3% of the area of the site (see Figure 4 left).

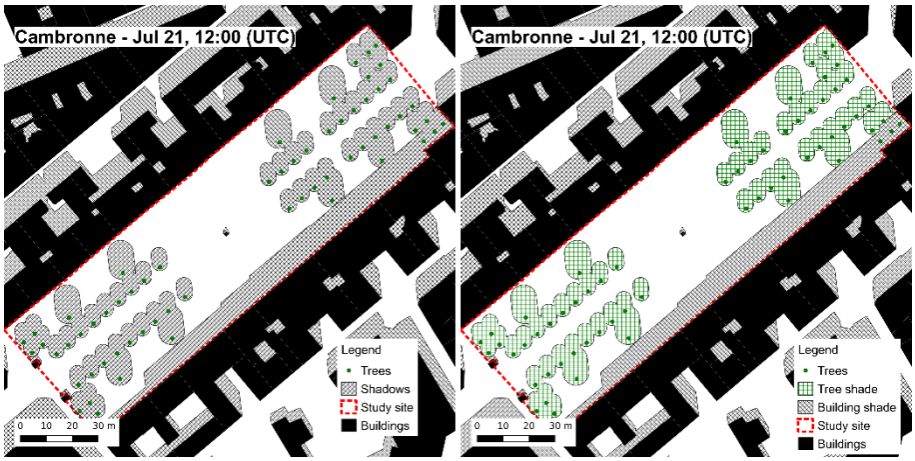

Figure 4. (left) The plugin allows evaluating both shadows of buildings and trees on a horizontal plane according to the date and time chosen. The result is a multi-polygon geometry (light-grey area). (right) The plugin is able to distinguish, in the shadow cast on the ground, the contribution of trees (light-green polygons) from that of buildings (light-grey polygons)

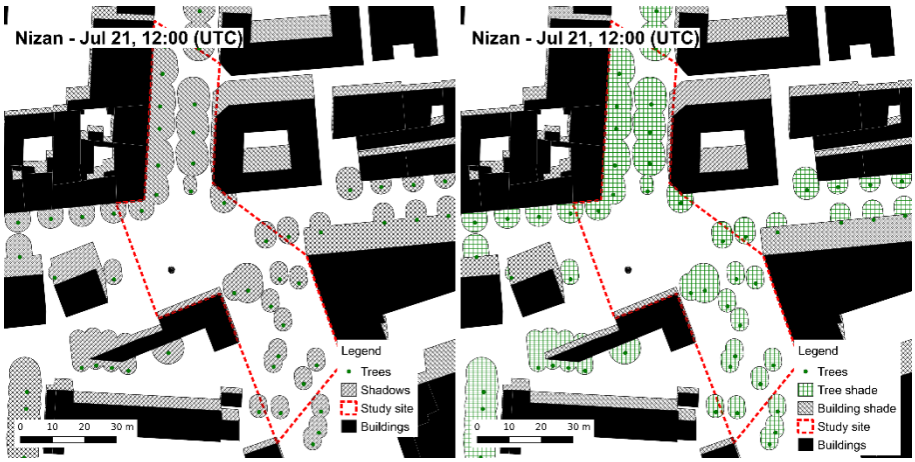

Figure 5. (left) The plugin shows that, at this 2nd site, the central square is highly exposed to solar radiation on July 21 at noon. For the area studied more precisely (red dotted line), the shadow is grouped at the 2 northern and southern ends. (right) The plugin shows that 93.8% of the shadow is of vegetation origin (the contribution of trees is represented by light-green polygons while that of buildings is represented by light-grey polygons)

By transposing the same method to the second site, we observe that the surrounding buildings and 24 trees enclosed in the study area around the Paul Nizan Street produce a shadow that covers 38.8% of the study area (see Figure 5 left).

5.1.2. Shade contribution of the tree canopy

In the context of urban greening policies, it is essential to distinguish the shadows generated by the built environment (*i.e.*, the buildings) from those produced by the tree canopy. For the configuration shown in Figure 4 (right), the shade produced by the tree canopy represents about 69.3% of the total shade on the ground. This proportion increases substantially in the second site where tree shade represents 93.8% of the total shade as shown in Figure 5 (right). This contribution is naturally conditioned by the tree crown geometries as well as by their spatial distribution within the urban space (they may indeed be hidden by possible taller buildings).

5.1.3. Shade ratio evolution over the summer period

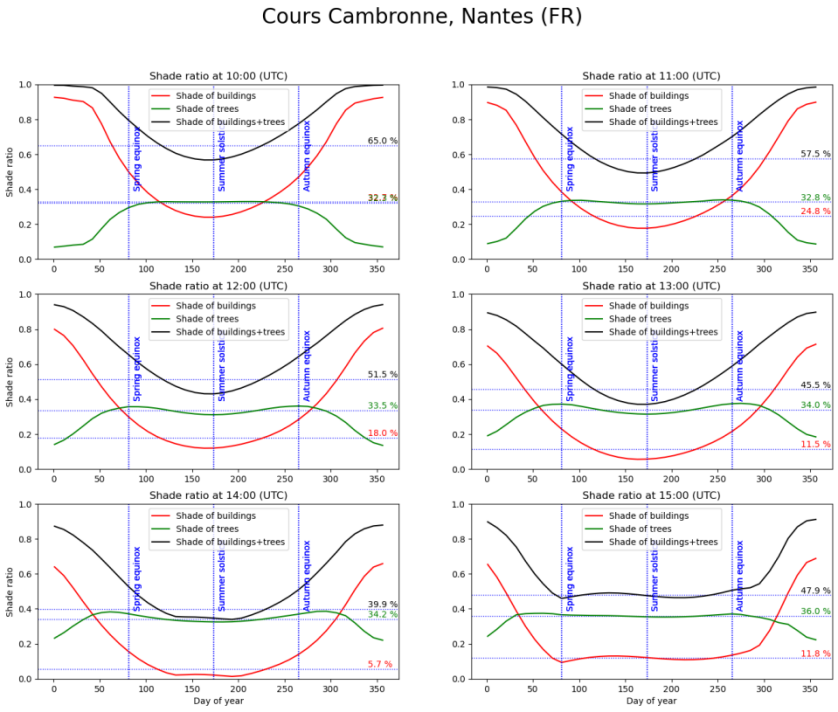

Figure 6. Evolution of shade ratios over the year for a few predetermined hours of daylight. The fall of foliage in autumn and winter is likely to modify the geometry of the crown and reduce the amount of shade

In this section, the yearly evolution of the shadow ratio for different times a day (between 10 a.m. and 4 p.m.) is studied. Figure 6 and 7 show that, without the shading provided by the tree canopy (*i.e.*, from the shading of the surrounding buildings alone), the two sites would present configurations that would consistently be more exposed to solar radiation.

If we decide to zoom on the hottest period (during summertime or around summer), when the sun is at its highest in the sky and, consequently, the solar energy input is the greatest. Considering the results in the first study site (Figure 6), for the period between spring equinox and autumn equinox, one can note that the tree shades cover on average one third of the courtyard. This contribution is almost systematically higher than the one of the surrounding buildings. At its peak (at 2 p.m. UTC), it is even around six times higher than the shade provided by the buildings.

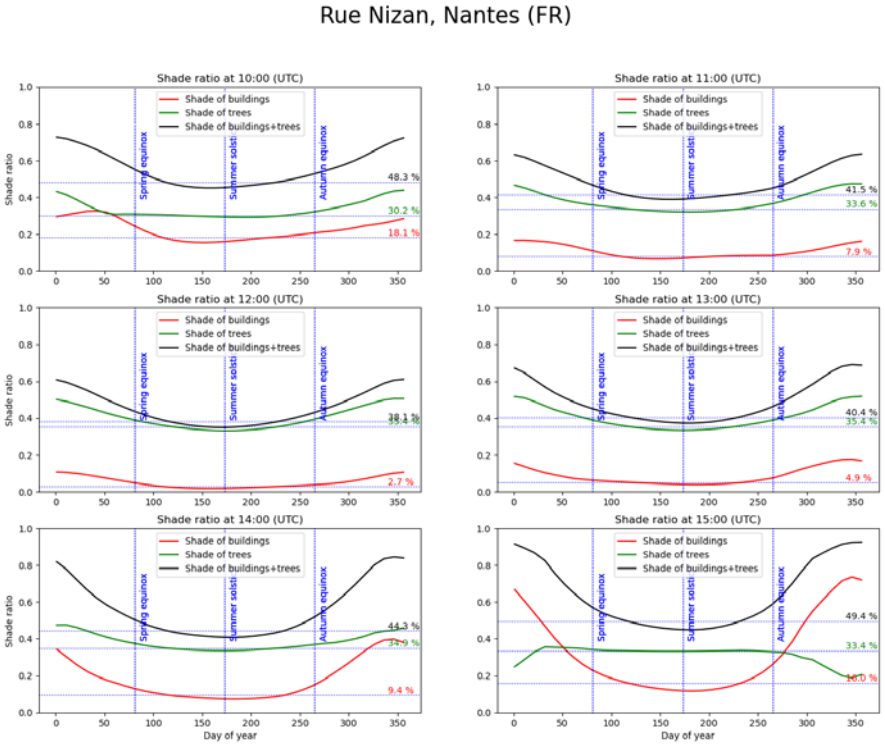

Figure 7. We note that, in this second site, even more than in the previous one, the contribution of shade from the tree canopy during the meridian hours is ultra-majoritarian. It is important to mention here that these hours are also those when the sun is at its highest in the sky and its energy contribution is at its maximum

Again, by transposing the same method to the second site, we observe that, between the spring and autumn equinoxes when the trees are in leaf, their contribution to shade systematically covers more than 30% of the ground surface of the site whatever the time of the day or the day itself (see Figure 7).

5.2. Shadowing permanence

5.2.1. Delineation of shaded areas over several hours

The annual evolution of the ground shade presented in the previous section can also be studied for a given day. This allows distinguishing potential cool spots, during a heat wave event. Thus, the shade zones are cut out according to the number of hours of shade. With the special case of September 14, 2020[5], Figure 8 (left) shows the excessively fragmented nature of this cut within the shadow zone of the first site. Nevertheless, the constituted puzzle differs substantially from that of July 21 presented in (Leduc *et al.*, 2021, Figure 5), where the central part near the statue was clearly more exposed to the sun. It can be seen, however, that although the central strip situated halfway between the two rows of trees (longitudinal centre line of the courtyard) is finally fairly exposed, the tree roots are very well protected.

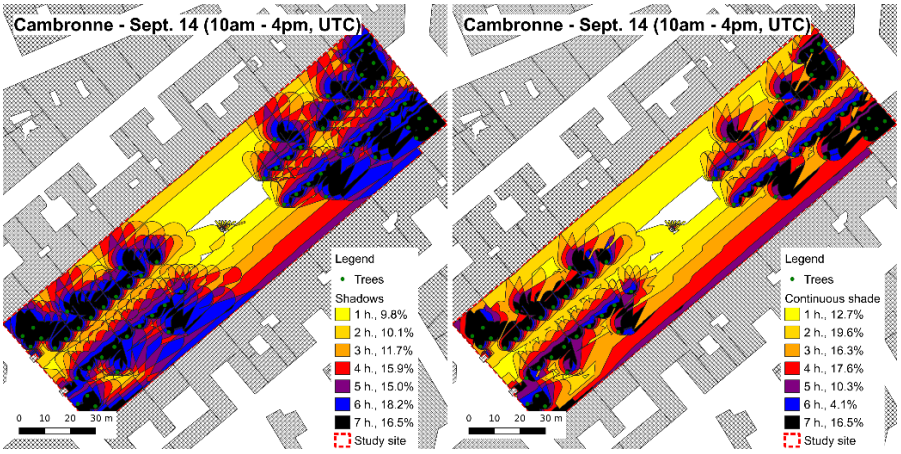

Figure 8. (left) Non-uniform distribution of shade in the courtyard during the daylight hours as the autumn equinox approaches. (right) Representation of areas in shade over several consecutive hours

In the case of the second site, the study of the shadow dynamics during this mid-September day shows less complexity in the sense that the equilibria and main trends remain relatively unchanged (see Figure 9 left). Thus, despite the variation in

5. On the same day, we carried out measurements on the Cambronne site as mentioned above.

the apparent position of the sun in the sky, the centre of the study area remains massively exposed to solar radiation. In contrast, the shading of the northern part of the site remains as dense as ever, forming a kind of permanent shadow canyon. In the southern part of the site, the evolution of the shadow patterns during the day does not allow the creation of a corridor guaranteeing permanent shade.

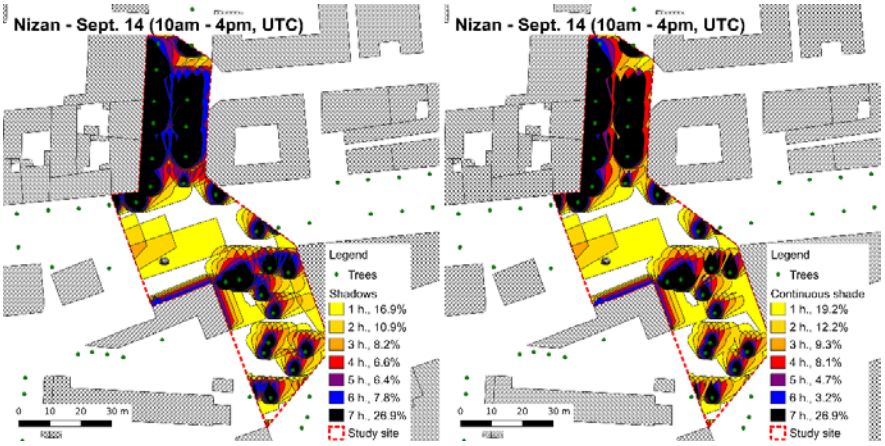

Figure 9. (left) Non-uniform distribution of shade in the site named Nizan during the daylight hours as the autumn equinox approaches. (right) Representation of areas in shade over several consecutive hours. The shading of the northern part of the site forms a sort of canyon of permanent shade

5.2.2. Delineation of shaded areas over several consecutive hours

The accumulation of shadow hours shown in Figure 8 (left) and in Figure 9 (left) does not include any notion of temporal continuity. However, it could be interesting to detect areas that are permanently in the shade (in order, for example, to design and deploy appropriate street furniture). Figure 8 (right) and Figure 9 (right) show a revised version of the indicator incorporating this dimension of continuity. The idea here is to represent areas as a function of their exposure to shade for several consecutive hours. As one can note, the overall fragmentation is much less, and patterns emerge that guarantee a certain spatial continuity.

5.2.3. Attempting to identify fresh corridors using cumulative comfort indexes

In this section, we ask ourselves whether the simulation results correlate with the measurements collected in situ during the five runs made on September 14, 2020. To this end, it seems that the PET (Höppe, 1999) calculated at any point along the pathway at various times of the day is a good indicator for revealing the accumulation of sun exposure. This thermal comfort index depends, among other parameters, on the mean radiant temperature – derived from the radiation balance. Although the measurements fluctuate and show more variability than the simulation

would predict, three main areas stand out (Figure 10). The first corresponds to the first 73 m of the path between the two rows of trees (between markers 31 and 32). In this zone, which is in the shade half the time, the average PET value is 37.5°C. From this area between the two rows of trees to marker 34, the course is very exposed to sunlight. The average PET value rises up to 44.3°C. It falls back to 33.1°C in a few metres beyond marker 34 as soon as the sensors reach an area of almost continuous shade. These three averages confirm the trends exhibited by our simulation tools.

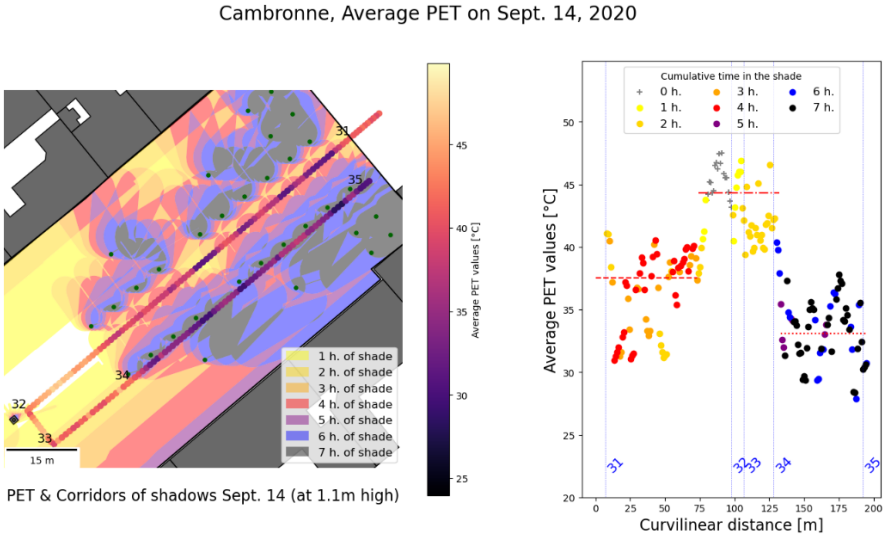

Figure 10. Superposition of the shadow continuities and the average values of the PET thermal comfort indicator derived from in situ measurement. The spatial correlation between the shadiest areas and the low PET values (left) is supported by the difference between the three PET averages (right)

6. Discussion

6.1. Pros: beyond descriptive analysis, shadow as a design object

While it is possible to vectorise the raster shadows obtained via UMEP, the underlying pixelisation is nevertheless problematic when seeking to use shadows for the design of urban spaces as given, for example, in the solar envelope concept (Knowles, 2003). From this point of view, our proposal is innovative in the specific context of geomatics as these vector shadows enable to delineate potential cool-paths and urban oases or cool spots in the urban fabric… all useful features for citizens during heat waves.

6.2. Contras: need for an energy-based approach

It should be noted, however, that the current method is not based on Digital Elevation Models (DEMs); thus, the interactions between the topography and the sun path model are not considered. This has many advantages over using a CityGML model of LoD 2 or higher. For instance, overlaying a terrain model composed of irregular triangles with different facets of walls and roof slopes complicates and lengthen the shadow calculation. By doing so, each triangle would need to be considered separately in order 1) to identify the various contributions of the neighbourhood in terms of cast shadows, 2) to carry out the geometrical union of the traces at each time step, and 3) to group the zones sharing the same shadow duration to draw the corridors.

However, this simplified approach has a downside. This is a potential application limit especially for cities with significant elevation changes. Furthermore, the simplified and strictly geometric approach is not sufficient to inform properly the complex notion of pedestrian thermal comfort in heterogeneous urban spaces. On the one hand, particular building geometries (*e.g.*, walkways, porches, steep rooftops) are not considered. On the other hand, thermal comfort simulation tools such as ENVI-met allow studying the spatial distribution of thermal comfort indexes by integrating an energy-based approach. Supplementing our tool with a more representative geometric approach, based on 3D city models (ex. CityGML, *cf.* Biljecki *et al*., 2018) and a thermo-radiative (or even aeraulic) model would make it possible to transform this prototype into a more relevant tool for city designers. Such an assessment will require considering the radiative models of the facades in a full 3D approach.

7. Conclusion

This article is a contribution to the bioclimatic analysis of outdoor urban spaces in the framework of applied geomatics. More precisely, it consists of the development of a vectorial solution for the calculation of the vegetal and mineral shadows. These shadow plots being themselves vector objects, this solution allows – from standard topographic datasets – to quantify the shadow part of a given place, to evaluate the evolution of the shadow cover during a day, a given summer period or even the whole year. As these shadow plots are time-stamped, it is also possible – by means of spatio-temporal queries – to identify shaded areas over several hours (consecutive or not) of the day and thus to delimit possible coolness reservoirs or shadow corridors.

This tool for a local authority-planning department is deliberately a standard geomatics tool. As such, it is based on a simple model for calculating shadows. Using a set of right prisms (buildings) and a set of point positions of trees (modelled by the superposition of a cylinder and a sphere or a cone trunk), as well as the apparent position of the sun in the sky, each building or vegetal mask is projected in

the horizontal plane. This projection allows handling the shadows as a set of 2D polygons and exploiting the powerful operators from the Geopandas library. Grouping the set of shadows projected in the single projection plane can be done by a single call to the "unary_union" operator.

Finally, our work contributes to a geomatics estimation of tree-shaded zones to building ones, which is crucial for summer thermal comfort. It also makes it possible to go beyond the calculation and descriptive analysis of the shadows cast in the urban space and to use them as standard polygonal shapes. Continuing its development by integrating a comprehensive energy and a more realistic geometric model will make it operational for urban planners.

Acknowledgment

This study is supported by the French National Research Agency (ANR) under reference ANR-18-CE22-0003 (COOLSCAPES project).

References

Abdel-Aziz D. M., Shboul A. Al, Al-Kurdi N. Y. (2015). Effects of Tree Shading on Building's Energy Consumption –The Case of Residential Buildings in a Mediterranean Climate. *American Journal of Environmental Engineering*, vol. 5, n° 5, p. 131-140

Aleksandrowicz O., Zur S., Lebendiger Y., Lerman Y. (2020). Shade maps for prioritizing municipal microclimatic action in hot climates: Learning from Tel Aviv-Yafo. *Sustainable Cities and Society* 53, September 2019, 101931, https://doi.org/10.1016/j.scs.2019.101931

Altman D. G., Bland J. M. (1994). Statistics Notes: Diagnostic Tests 1: Sensitivity and Specificity. *BMJ*, vol. 308, n° 6943, p. 1552-1552, https://www.bmj.com/lookup/doi/10.1136/bmj.308.6943.1552.

Aram F., Higueras García E., Solgi E., Mansournia S. (2019). Urban green space cooling effect in cities. *Heliyon*, vol. 5, n° 4, e01339, https://doi.org/10.1016/j.heliyon.2019.e01339

Biljecki F., Kumar K., Nagel C. (2018). CityGML Application Domain Extension (ADE): overview of developments. *Open Geospatial Data, Software and Standards*, vol. 3, n° 1, p. 13, https://opengeospatialdata.springeropen.com/articles/10.1186/s40965-018-0055-6

Coutts A. M., White E. C., Tapper N. J., Beringer J., Livesley S. J. (2016). Temperature and human thermal comfort effects of street trees across three contrasting street canyon environments. *Theoretical and Applied Climatology*, vol. 124, n° 1-2, p. 55-68, http://link.springer.com/10.1007/s00704-015-1409-y

Cui L., Rupprecht C. D. D., Shibata S. (2021). Climate-responsive green-space design inspired by traditional gardens: Microclimate and human thermal comfort of Japanese gardens. *Sustainability*, vol. 13, n° 5, p. 2736, https://www.mdpi.com/2071-1050/13/5/2736

Davis L. W., Gertler P. J. (2015). Contribution of air conditioning adoption to future energy use under global warming. *Proceedings of the National Academy of Sciences* vol.112, n° 19, p. 5962–5967, http://www.pnas.org/lookup/doi/10.1073/pnas.1423558112

Demuzere M., Orru K., Heidrich O., Olazabal E., Geneletti D., Orru H., Bhave A. G., Mittal N., Feliu E., Faehnle M. (2014). Mitigating and adapting to climate change: Multi-functional and multi-scale assessment of green urban infrastructure. *Journal of Environmental Management* 146, p. 107-115, https://linkinghub.elsevier.com/retrieve/pii/S0301479714003740

Emmanuel R., Loconsole A. (2015). Green infrastructure as an adaptation approach to tackling urban overheating in the Glasgow Clyde Valley Region, UK. *Landscape and Urban Planning* 138, p. 71-86, https://linkinghub.elsevier.com/retrieve/pii/S0169204615000432

Ewing R., Handy S., Brownson R. C., Clemente O., Winston E. (2006). Identifying and measuring urban design qualities related to walkability. *Journal of Physical Activity and Health* vol. 3(Suppl 1), p. 223-240, http://forum.activelivingresearch.com/sites/default/files/JPAH_15_Ewing.pdf

Feyisa G. L., Dons K., Meilby H. (2014). Efficiency of parks in mitigating urban heat island effect: An example from Addis Ababa. *Landscape and Urban Planning*, 123, p. 87-95, http://dx.doi.org/10.1016/j.landurbplan.2013.12.008

Gehl J., (2011). *Life Between Buildings: Using Public Space*, Island Press/Center for Resource Economics.

Gillies S., Taves M., Arnott J., Tonnhofer O., Bossche J. Van den, Wasserman J., Bierbaum A., Caruso T., *et al.* (2021). *Toblerity/Shapely: Shapely 1.8.0*, https://doi.org/10.5281/zenodo.5597139

Gillner S., Vogt J., Tharang A., Dettmann S., Roloff A. (2015). Role of street trees in mitigating effects of heat and drought at highly sealed urban sites. *Landscape and Urban Planning*, 143, p. 33-42, http://dx.doi.org/10.1016/j.landurbplan.2015.06.005

Gunawardena K. R, Wells M. J., Kershaw T. (2017). Utilising green and bluespace to mitigate urban heat island intensity. *Science of The Total Environment*, n° 584-585, p. 1040-1055, http://dx.doi.org/10.1016/j.scitotenv.2017.01.158

Gupta A. K., Skog I., Handel P. (2015). Long-term performance evaluation of a foot-mounted pedestrian navigation device. *2015 Annual IEEE India Conference (INDICON)*, p. 1-6, http://ieeexplore.ieee.org/document/7443478/

Hansen J., Sato M., Hearty P., Ruedy R., Kelley M., Masson-Delmotte V, Russell G., Tselioudis G., Cao J., Rignot E., Velicogna I., Tormey B., Donovan B., Kandiano E., *et al.* (2016). Ice melt, sea level rise and superstorms: Evidence from paleoclimate data, climate modeling, and modern observations that 2 °C global warming could be dangerous. *Atmospheric Chemistry and Physics*, vol. 16, n° 6, p. 3761-3812, https://www.atmos-chem-phys.net/16/3761/2016/

Hawkins E. (2018). Warming stripes. *Climate Lab Book*. U.K, http://www.climate-lab-book.ac.uk/2018/warming-stripes/

Höppe P. (1999). The physiological equivalent temperature - A universal index for the biometeorological assessment of the thermal environment. *International Journal of Biometeorology* vol. 43, n° 2, p. 71-75 http://www.embase.com/search/results?subaction=viewrecord&from=export&id=L12934 7950

IGN (2021a). BD TOPO®, https://geoservices.ign.fr/bdtopo

IGN (2021b). RGE ALTI®, https://geoservices.ign.fr/rgealti

IPCC (2022). The Ocean and Cryosphere in a Changing Climate (Cambridge University Press), https://www.ipcc.ch/report/srocc/

Johansson E., Thorsson S., Emmanuel R., Krüger E. (2014). "Instruments and methods in outdoor thermal comfort studies – The need for standardization. *Urban Climate*, 10(P2), p. 346-366, https://linkinghub.elsevier.com/retrieve/pii/S221209551300062X

Jordahl K., Bossche J Van den, Fleischmann M., McBride J., Wasserman J., Badaracco A. G., Gerard J., Snow A. D., *et al.* (2022). "geopandas/geopandas: v0.11.0", https://doi.org/10.5281/zenodo.2585848

Kabisch N., van den Bosch M., Lafortezza R. (2017). The health benefits of nature-based solutions to urbanization challenges for children and the elderly – A systematic review. *Environmental Research*, 159, July, p. 362-373 https://linkinghub.elsevier.com/retrieve/pii/S0013935117315396

Knowles R. L. (2003). The solar envelope: its meaning for energy and buildings. *Energy and Buildings* vol. 35, n° 1, p. 15-25 http://linkinghub.elsevier.com/retrieve/pii/S0378778802000762 , p.

Lafortezza R., Chen J., van den Bosch C. K., Randrup T. B. (2018). Nature-based solutions for resilient landscapes and cities. *Environmental Research* 165, December 2017, p. 431-441, https://linkinghub.elsevier.com/retrieve/pii/S0013935117317115

Leduc T., Stavropulos-Laffaille X., Requena Ruiz I. (2021). Implementation of a solar model and shadow plotting in the context of a 2D GIS: challenges and applications for the cooling effect of tree-covered based greening solutions in urban public spaces, *SAGEO 2021, 16th Spatial Analysis and Geomatics Conference*, Eds P.-A. Davoine, D. Josselin, and F. Pinet (UMR 7300 ESPACE, La Rochelle, France), p 89-100, http://sageo2021.univ-lr.fr/

Leduc T. (2022). "t4gpd", https://zenodo.org/record/5782942

Lindberg F., Grimmond C. S. B., Gabey A., Huang B., Kent C. W., Sun T., Theeuwes N. E., Järvi L., Ward H. C., Capel-Timms I., Chang Y., Jonsson P., Krave N., Liu D., Meyer D., Olofson K. F. G., Tan J., Wästberg D., Xue L., Zhang Z. (2018). Urban Multi-scale Environmental Predictor (UMEP): An integrated tool for city-based climate services. *Environmental Modelling & Software*, 99, p. 70-87, https://linkinghub.elsevier.com/retrieve/pii/S1364815217304140

Martilli A., Krayenhoff E. S., Nazarian N. (2020). Is the Urban Heat Island intensity relevant for heat mitigation studies? *Urban Climate* 31, (January 2019) 100541, https://linkinghub.elsevier.com/retrieve/pii/S2212095519300070

Middel A., Selover N., Hagen B., Chhetri N. (2016). Impact of shade on outdoor thermal comfort. A seasonal field study in Tempe, Arizona. *International Journal of Biometeorology*, vol. 60, n° 12, p. 1849-1861, http://dx.doi.org/10.1007/s00484-016-1172-5

Miguet F., Groleau D. (2002). A daylight simulation tool for urban and architectural spaces. Application to transmitted direct and diffuse light through glazing. *Building and environment*, 37, p. 833-843. http://www.sciencedirect.com/science/article/pii/S0360132302000495

Mullaney J., Lucke T., Trueman S. J. (2015). A review of benefits and challenges in growing street trees in paved urban environments. *Landscape and Urban Planning*, 134, p. 157-166, https://linkinghub.elsevier.com/retrieve/pii/S016920461400245X

QGIS Association (2022). *QGIS Geographic Information System*, https://www.qgis.org

Redon E., Lemonsu A., Masson V. (2020). An urban trees parameterization for modeling microclimatic variables and thermal comfort conditions at street level with the Town Energy Balance model (TEB-SURFEX v8.0). *Geoscientific Model Development* 13, n° 2, p. 385-399, https://gmd.copernicus.org/articles/13/385/2020/

Requena-Ruiz I., Siret D., Stavropulos-Laffaille X., Leduc T. (2023). Designing thermally sensitive public spaces: An analysis through urban design media. *Journal of Urban Design*, vol. 28, n° 1, p. 44-65, https://doi.org/10.1080/13574809.2022.2062312

Rhodes B. C. (2011). *PyEphem: Astronomical Ephemeris for Python*. https://ui.adsabs.harvard.edu/abs/2011ascl.soft12014R

Roudsari M. S., Pak M. (2013). Ladybug: A parametric environmental plugin for grasshopper to help designers create an environmentally-conscious design. *Proceedings of BS 2013: 13th Conference of the International Building Performance Simulation Association*, p. 3128-3135

Ruefenacht L. A., Acero J. A (2017). *Strategies for Cooling Singapore: A catalogue of 80+ Measures to Mitigate Urban Heat Island and Improve Outdoor Thermal Comfort*, https://www.research-collection.ethz.ch/handle/20.500.11850/258216

Seager R., Osborn T. J., Kushnir Y., Simpson I. R., Nakamura J., Liu H. (2019). Climate Variability and Change of Mediterranean-Type Climates. *Journal of Climate*, vol. 32, n° 10, p. 2887-2915, https://journals.ametsoc.org/jcli/article/32/10/2887/317/Climate-Variability-and-Change-of

Sobstyl J. M., Emig T., Qomi M. J. A., Ulm F.-J., Pellenq R. J.-M. (2018). Role of City Texture in Urban Heat Islands at Nighttime. *Physical Review Letters*, vol. 120, n° 10, p. 108701, https://link.aps.org/doi/10.1103/PhysRevLett.120.108701

Stafford B. (2020). *Pysolar*, https://doi.org/10.5281/zenodo.5518074

Stavropulos-laffaille X., Requena-Ruiz I. (2021). Urban cooling strategies as interaction opportunities in the public space: A methodological proposal. *Coolscapes*, https://coolscapes.hypotheses.org/535

Taha H., Akbari H., Rosenfeld A., Org E. (1991). Heat island and oasis effects of vegetative canopies: Micro-meteorological field-measurements theoretical and applied climatology

theoretical and applied climatology, 44, p. 123-138, https://escholarship.org/uc/item/5wt7072h

Whyte W H. (1980). *The Social Life of Small Urban Spaces*, Washington, D.C: Conservation Foundation.

Yin L. (2017). Street level urban design qualities for walkability: Combining 2D and 3D GIS measures. C*omputers, Environment and Urban Systems* 64, p. 288-296, http://dx.doi.org/10.1016/j.compenvurbsys.2017.04.001